Photoinduced Intramolecular Electron Transfer in Phenylene Ethynylene Naphthalimide Oligomers

Yajing Yang,[a,b,†] Silvano R. Valandro,[b,†] Zhiliang Li,[a,b] Soojin Kim[b] and Kirk S. Schanze[b,*]

[a]University of Florida, Department of Chemistry, P.O. Box 117200, Gainesville, FL, 32611

[b]University of Texas at San Antonio, Department of Chemistry, One UTSA Circle, San Antonio, TX 78249

* Corresponding author email: kirk.schanze@utsa.edu

† Equal Contributions

Abstract

This paper reports a photophysical investigation of a series of phenylene ethynylene oligomers (OPE) that are end-substituted with a 1,8-naphthalene imide (NI) acceptor. The NI acceptor is attached to the terminus of the phenylene ethynylene oligomers *via* an ethynylene (-C≡C-) unit that is linked at the 4-position of the NI unit. A series of three oligomers is investigated, OPE1-NI, OPE3-NI and OPE5-NI, which contain 1, 3 and 5 phenylene ethynylene repeat units, respectively. The properties of the OPEn-NI series are compared to a corresponding set of unsubstituted OPEs, OPE3 and OPE5, which contain 3 and 5 phenylene ethynylene repeats, respectively. The photophysics of the all of the compounds are interrogated by a variety of techniques including steady-state absorption, steady-state fluorescence, 2-photon absorption, time-resolved fluorescence and transient absorption spectroscopy on femtosecond to microsecond timescales. The effect of solvent polarity on the properties of the oligomers is examined. The results show that the NI-substituted oligomers feature a lowest charge transfer (CT) excited state, where the OPE segment acts as the donor and the NI moiety is the acceptor ($OPEn^{\bullet+}$-$NI^{\bullet-}$). The absorption spectra in 1-photon and 2-photon exhibit a clear manifold of absorption features that can be attributed to direct CT absorption. In moderately polar solvents, the emission is dominated by a broad, solvatochromic band that is due to radiative decay from the CT excited state. Ultrafast transient absorption provides evidence for initial population of a locally excited state (LE) which in moderately polar solvents rapidly (~1 ps) evolves into the CT excited state. The structure, spectroscopy and dynamics of the CT state is qualitatively similar for OPE3-NI and OPE5-NI, suggesting that delocalization in the OPE segment does not have much effect on the structure or energetics of the CT excited state.

Introduction

Electron transfer (ET) is a fundamental step involved in important chemical and biological processes, such as light-harvesting, energy conversion and energy storage.[1-5] Electron transfer and charge transport in organic conjugated materials are essential processes in the function of organic solar cells and other organic electronic devices.[6-7] As such, theoretical and experimental research on photoinduced ET in π-conjugated molecules (e.g., donor-bridge-acceptor systems) have been conducted to improve understanding of the mechanism that controls this process.[1, 8-21]

A variety of π-conjugated "molecular wires" have been designed to study the ET process, including systems containing oligofluorene,[22] oligothiophene,[23] oligo-phenylenevinylene,[24] and oligo(phenylene ethynylene) (OPE)[25] as a bridge. Despite considerable efforts on these π-conjugated molecules, most of the reports, especially on OPE-based systems, have been limited to using the conjugated segments as bridges between donor and acceptor moieties. There is much less research on molecules where the conjugated segment acts as the electron donor and is linked to an acceptor.[23, 26] Interest in these systems comes from the need to understand the effect of conjugation length and delocalization on the charge separation and recombination processes. These effects are relevant to the primary steps in charge carrier generation in organic solar cells.[27] In previous work we and others have explored acceptor-substituted conjugated oligomers featuring fullerene[28-30] or diimide acceptors[23, 26, 31]. In most cases, the oligomer-acceptor systems are weakly coupled, and therefore photoinduced and return ET occur via non-adiabatic pathways. Due to the weak coupling, direct radiative decay of the charge separated state (via charge transfer emission) is not observed. However, several recent reports have shown that by use of the 1,8-naphthaleneimide (NI) acceptor on oligofluorenes and oligothiphenes gives rise to donor-acceptor systems where charge transfer (CT) emission is observed.[32-36]

Herein, we report the synthesis and photoinduced electron transfer investigation of a series of oligo(phenylene ethynylene)s that are capped with a 1,8-naphthalimide electron acceptor (OPEn-NI). The effects of length of the OPE segment and solvent polarity on the dynamics of photoinduced charge separation and recombination were investigated. For this purpose, the OPE segment length was varied, with n = 1, 3 and 5 (Chart 1). Changing the length of the oligophenylene ethynylene changes the energetics and the structure/delocalization of the charge separated state. In contrast to work previously reported for the related OPEs substituted with a weakly coupled naphthalene diimide acceptor,[26] incorporating the NI group as an acceptor gives rise to systems with strong emission from a CT state, thus facilitating spectroscopic characterization. The experimental findings from the OPEn-NI compounds reveal the strong impact of donor chain length and solvent properties have on the ET rates.

Chart 1. Structures of OPEn (n=3 and 5) and OPEn-NI (n=1, 3 and 5) oligomers.

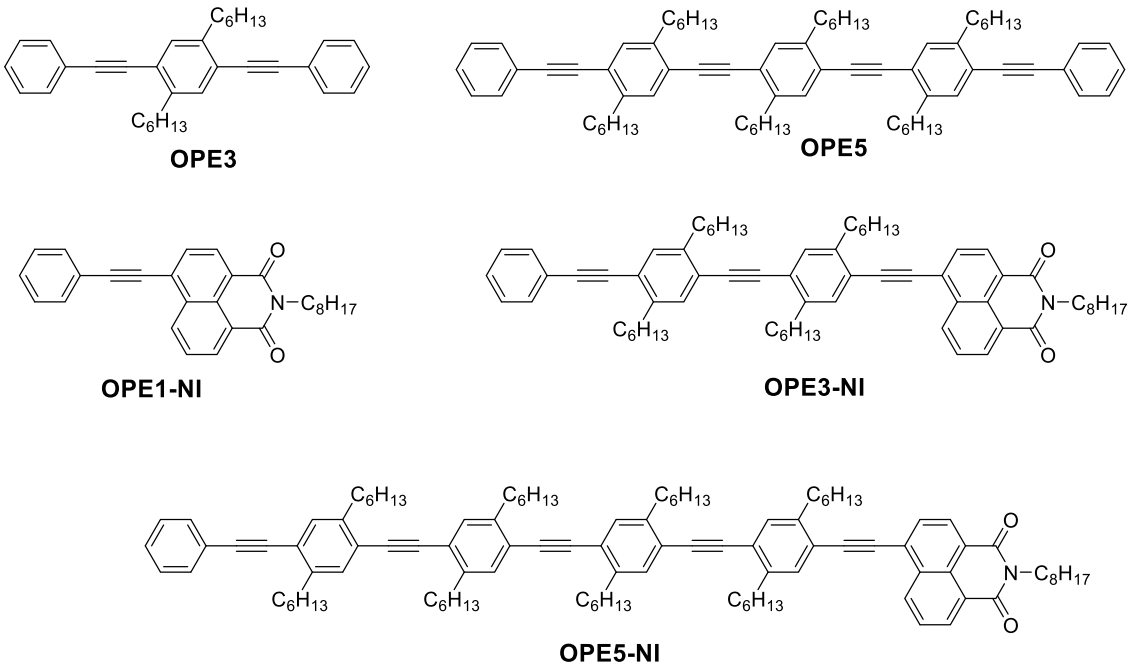

Experimental Section

Instrumentation and Methods. ^{1}H and ^{13}C NMR spectra were recorded on Inova2 (500 MHz) and Bruker Ascend TM (300MHz and 500MHz) spectrometers in $CDCl_3$. Chemical shifts (δ) were reported in parts per million (ppm) using $CDCl_3$ as solvents and were referenced to residual solvent peaks. High-resolution mass spectrometry was performed with a Bruker Daltonics Ultraflextreme MALDI-TOF/TOF mass spectrometer in the Chemistry Department at the University of Texas, San Antonio.

UV-Visible spectra were acquired on a Shimadzu UV-1800 dual beam absorption spectrophotometer. Photoluminescence spectra were recorded on an Edinburgh Instruments FLS 1000. Fluorescence lifetimes were collected Time-Correlated Single Photon Counting (TCSPC) technique in a PicoQuant FluoTime 300 Fluorescence Lifetime Spectrophotometer (PicoQuant PicoHarp 300 module). A Ti:Saphire laser (Coherent Chameleon Ultra) was used as excitation source. The Chameleon laser provides pulses of 80 MHz, which were sampled using a Coherent Model 9200 pulse picker to provide excitation pulses at 4000 kHz repetition rate and was frequency doubled using a Coherent second harmonic generator. Excitation wavelength of 340 and 370 nm were chosen for the oligomers and the instrument response function (IRF) was measured by using a Ludox scattering solution. The concentration of OPEnNI solution was 10^{-6} M.

The 2PA measurements were obtained by two-photon-induced fluorescence technique.[37] A Coherent Chameleon Ultra Ti:Saphire laser was used as excitation source. The signal beam wavelength was tunable from λ_{ex} = 680 to 1000 nm. The pulse energy was adjusted by passing the beam through an achromatic half-wave plate (Thorlabs) and polarizing beamsplitter cube (Thorlabs). The samples were placed behind a f = 12.5 cm focusing lens. The fluorescence spectra were collected in Photon Technology International (PTI) spectrophotometer. The 2PA spectra

were obtained by measuring the intensity of the two-photon excited fluorescence spectrum as a function of the excitation wavelength and normalized to the square of the power at the specific excitation wavelength. The relative 2PA spectra were correct to absolute cross-section.[38] The absolute 2PA cross-section were determined using the equation 1 and the BDPAS as reference standard. [39]

$$\sigma_{2,s} = \frac{F_{2,s}(\lambda_{reg})C_r\eta_r(\lambda_{reg})}{F_{2,r}(\lambda_{reg})C_s\eta_s(\lambda_{reg})}\sigma_{2,r} \quad (1)$$

where σ_2 is the two-photon cross section, $F_2(\lambda_{reg})$ is the two-photon excited fluorescence intensity at a specific registration wavelength, C_r is the concentration, and $\eta(\lambda_{reg})$ is the absorbance corrected differential quantum efficiency at a specific registration wavelength. In equation 8, the subscripts *s* and *r* refer to the sample and reference, respectively. The concentrations used for the calculation were obtained from Beer's Law. The absorbance-corrected differential quantum yield was calculated according equation 2.

$$\left(\lambda_{reg}\right) = \frac{F_1(\lambda_{reg})}{A(\lambda_{exc})} \quad (2)$$

where *A* is the absorbance at the excitation wavelength and $F_1(\lambda_{reg})$ is the one-photon fluorescence intensity at the registration wavelength.

Nanosecond transient absorption spectroscopy measurements were collected in LP980 Spectrometer (Edinburgh Instruments) combined with a Continuum Surelite series Nd:YAG laser (λ_{ex}=355 nm, 10 ns fwhm and 4 mJ/pulse). Transient studies were carried in HPLC grade tetrahydrofuran (THF) and 1:3 acetronitrile/THF mixtures for the intermolecular charge transfer experiment. Oligomers concentrations were adjusted to give an optical density ≈0.6, at 355 nm. The samples were deoxygenated for 30 nm prior the measurements. Triethylamine (TEA) was

used as electron acceptor in the intermolecular charge transfer experiment at a concentration of 5 mM.

Femtosecond time-resolved transient absorption spectroscopy (fs-TA) measurements were performed using a broadband (350-1600 nm) pump-probe femtosecond transient absorption spectrometer HELIOS, Ultrafast Systems equipped with UV-visible and near-IR detectors. An amplified femtosecond Ti:Sapphire laser system (Astrella, Coherent, Inc.) displaying at 800nm with pulse width of 100 fs and 1 kHz repetition rate coupled with an optical paramagnetic amplifier (Coherent) was used for pulse pump generation. Probe light in the visible and near-infrared was generated by passing a small portion of the 800 nm light from the Ti:Sapphire laser through a computerized optical delay and focusing in a sapphire plate or a proprietary crystal to generate white-light continuum (VIS and NIR). The sample solutions were constantly stirred to avoid photodegradation. Transient absorption data were analyzed using global analysis and singular value decomposition (SVD) by Surface Xplorer PRO program from Ultrafast Systems.

Cyclic voltammetry (CV) and differential pulse voltammetry (DPV) were performed using a Bioanalytical Systems CV50W electrochemical analyzer at a sweep rate of 100 mV/s. The three-electrode setup consisted of two platinum wires as working and auxiliary electrodes and silver chloride/silver as reference electrode. Samples were prepared in dry dichloromethane with 0.1M tetrabutylammonium hexafluorophosphate as supporting electrolyte and degassed with nitrogen flow for 30 min before the measurements. Electrochemical potentials were calibrated against a ferrocene/ ferrocenium standard in dichloromethane.

Results and Discussion

Synthesis of Building Blocks and Designed Compounds. The series of oligo-phenylene ethynylene-naphthalimide compounds, OPEn-NI (*n* = 1, 3 and 5) and model compounds, OPEn (n = 3 and 5), were synthesized via Sonogashira coupling reactions. Complete details regarding the synthesis and characterization are given in Supporting Information. The NI acceptor was used in this investigation with the expectation that fluorescence from the OPE → NI charge transfer excited state would be observed. This expectation was based on previous work on a variety of π-conjugated chromophores that are substituted with the NI acceptor, including oligo- and polyfluorenes and oligothiophenes.[32-33, 36]

Linear Absorption and Photoluminescence Spectroscopy of OPEn and OPEn-NI Series. The photophysical properties of the OPEn and OPEn-NI compounds were studied in solvents with varying polarity and the results are summarized in Table 1. Figure 1 shows the absorption and fluorescence spectra of the two series of oligomers in three representative solvents: hexane, tetrahydrofuran (THF) and dichloromethane (DCM). Spectral data obtained in a more complete set of solvents with varying polarity are provided in the Supplementary Information. The OPEn series (n = 3 and 5) exhibit the typical spectral features of conjugated phenylene-ethynylene compounds, namely strong absorption in the UV-visible region and a narrow fluorescence feature accompanied by a vibronic band.[40-41] The absorption and fluorescence bands are red-shifted upon increasing the number of phenylene ethynylene units, but they show very little dependence on solvent, consistent with the lack of polar character in the ground and excited states.

The spectral features of OPEn-NI are clearly distinct from those of OPEn. The absorption spectrum of OPE3-NI (Figure 1g) exhibits two well-resolved absorption bands. The band at 330 nm is at a similar wavelength range compared to the OPE3 absorption peak, which is assigned to

be a locally excited (LE) absorption arising from the OPE segment. The longer wavelength absorption around 400 nm is due to a charge transfer (CT) absorption, since this band broadens and red shifts with increasing solvent polarity. The absorption spectrum of OPE5-NI (Figure 1i) features a single broad absorption band, due to the superposition of the LE and CT absorptions. Note that the long wavelength side of the absorption of OPE5-NI reveals a solvent dependence consistent with CT character.

As shown in Table 1, both OPE3 and OPE5 are strongly fluorescent with high fluorescence quantum yields. The fluorescence spectra of the OPEn series exhibit little change as the solvent polarity is increased. By contrast, upon increasing the solvent polarity, the fluorescence of the OPEn-NI oligomers broadens and red-shifts. This solvent dependence of the fluorescence is attributed to intramolecular charge transfer (CT) state emission. It should be noted that only a small shift in the maximum fluorescence wavelength was observed from OPE3-NI to OPE5-NI, suggesting that the charge-transfer in OPE5-NI is mainly localized in the first three or four OPE units linked to NI moiety. Note that for OPE3-NI and OPE5-NI, the fluorescence spectra not only displayed the CT characteristic peak at above 500 nm, but also exhibited a weak fluorescence band at higher energy (~400 nm) that resembled the corresponding OPEn emission spectrum. These features suggested that in the oligomers, both CT state and a LE state are emissive.

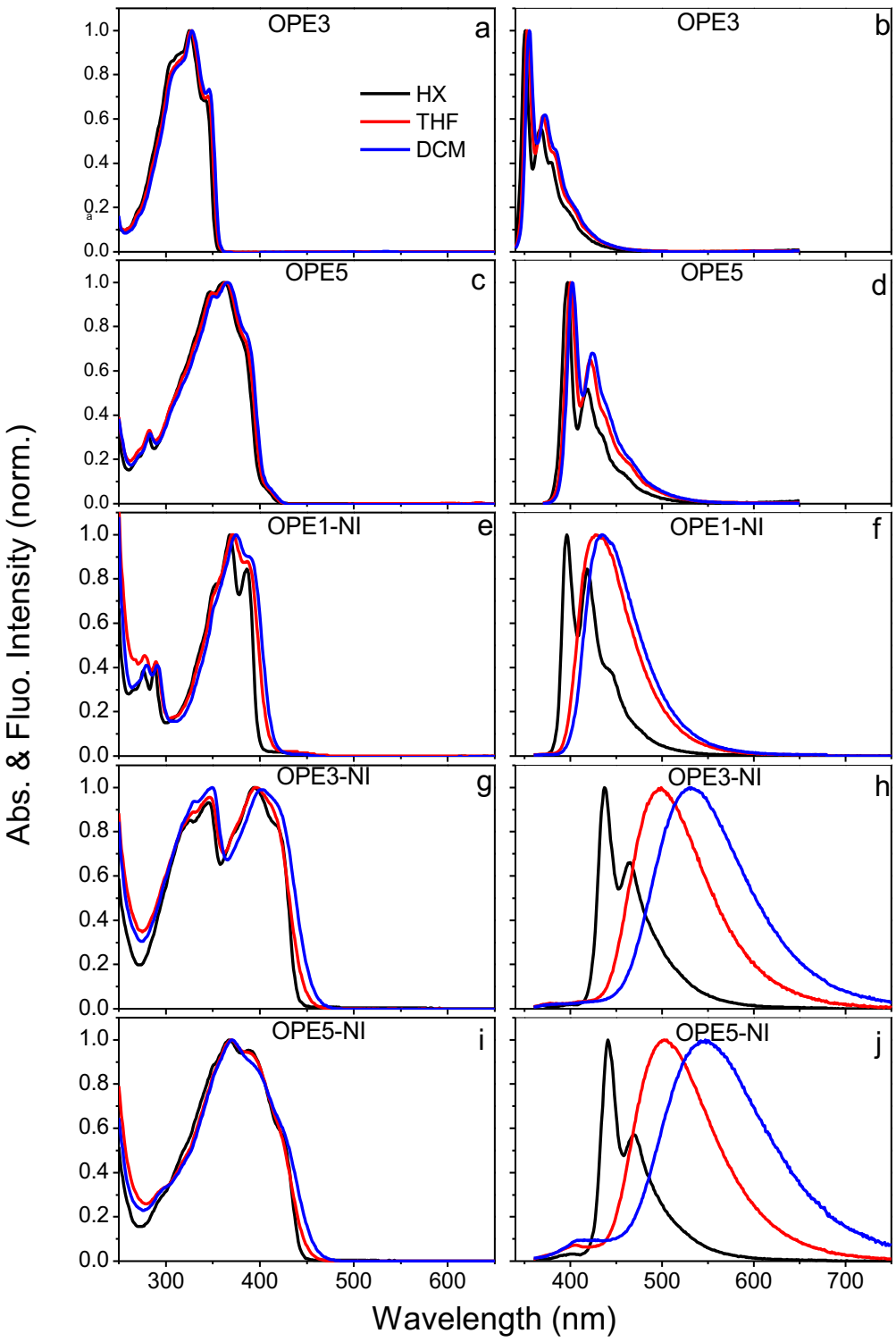

Figure 1. Optical spectra of oligomers in hexane (black), THF (red) and DCM (blue). (a) Absorption and (b) fluorescence spectra of OPE3. (c) Absorption and (d) fluorescence spectra of OPE5. (e) Absorption and (f) fluorescence spectra of OPE1-NI. (g) Absorption and (h) fluorescence spectra of OPE3-NI. (i) Absorption and (j) fluorescence spectra of OPE5-NI Samples were excited at 340 nm.

Fluorescence decay kinetics measurements were performed to study the dynamics in OPEn and OPEn-NI. The emission monitored at the respective band maxima indicate that OPEn series feature a mono-exponential decay attributed to the singlet excited state. An increase in the OPEn oligomer chain length leads to a slight decrease in the fluorescence lifetime (Table 1). Previous reports attributed this behavior to an increase in the radiative decay rate with oligomer length.[42-44] While no significant solvent effect in the fluorescence lifetime was observed for OPEn series, the situation is different with the inclusion of the NI moiety. The fluorescence decays for OPEn-NI series were fitted by a biexponential function, and the relative amplitude and lifetime of the components are affected by solvent polarity. The longer-lived decay component (τ_2) is clearly due to a CT state, as the amplitude and lifetime increases with solvent polarity.

Table 1. Summary of photophysical properties of OPEn and OPEn-NI oligomers.

Sample	Solvent	ε ($M^{-1}\cdot cm^{-1}$)	λ_{em}(nm)	Φ^a	$\tau_f{}^b$	
					τ_1 (ns)	τ_2(ns)
OPE3	hexane	1.3×10^5	351	0.83	0.67	-
OPE3	THF	4.8×10^4	353	0.63	0.70	-
OPE3	DCM	7.2×10^4	355	0.68	0.70	-
OPE5	hexane	1.5×10^5	397	0.70	0.57	-
OPE5	THF	1.6×10^5	400	0.71	0.60	-
OPE5	DCM	1.4×10^5	402	0.79	0.62	-
OPE1-NI	hexane	5.3×10^4	396	0.39	0.09 (0.2)	1.32 (0.8)
OPE1-NI	THF	3.6×10^4	429	0.40	0.11 (0.2)	1.58 (0.8)
OPE1-NI	DCM	4.9×10^4	435	0.48	0.27 (0.2)	1.65 (0.8)

OPE3-NI	hexane	4.2×10^4	438	0.27	0.29 (0.2)	1.32 (0.8)
OPE3-NI	THF	3.6×10^4	499	0.91	0.41 (0.1)	2.03 (0.9)
OPE3-NI	DCM	3.4×10^4	532	0.85	-	2.48
OPE5-NI	hexane	1.4×10^5	441	0.66	0.47 (0.2)	1.10 (0.8)
OPE5-NI	THF	5.8×10^4	503	0.64	0.73 (0.1)	1.90 (0.9)
OPE5-NI	DCM	1.7×10^5	546	0.51	0.63 (0.1)	2.37 (0.9)

[a]Fluorescence quantum yields were measured using quinine sulfate in 0.1 M sulfuric acid ($\Phi_F = 0.54$) as the reference. [b]Lifetimes were measured using time-correlated single photon counting (TCSPC) method, all the samples were excited at 340 nm and the decays were monitored at maximum fluorescence wavelength.

Two-Photon Absorption (2PA) Spectroscopy. Two-photon absorption (2PA) has been used to determine the changes in the dipole moment, $\Delta\mu$, in centrosymmetric and noncentrosymmetric chromophores.[45] Furthermore, 2PA can be a helpful tool to study the effect of solvents, conjugation length, and to aid assignment of charge-transfer transitions in D-A systems.[46-47] As such, we applied the two photon excited fluorescence method (2PEF) to measure the two-photon absorption (2PA) spectra of OPEn and OPEn-NI compounds in various solvents and the data are summarized in Figure 2.[37, 48-49] First, Figure 2a compares the 2PA spectra of OPEn and OPEn-NI in hexane solvent. Here it is seen that the OPEn series exhibit a single 2PA band around 690 nm and the cross-section σ_{2PA} increases with OPE chain length. This enhancement in the σ_{2PA} has been ascribed to an effective increase in π-delocalization due to increase in conjugation length.[49]

Secondly, as can also be seen in Fig. 2a, the OPEn-NI series exhibit two sets of 2PA bands: one with $\lambda \sim 690$ nm and a second series of bands in the range $\lambda \sim 750$ - 900 nm. More detailed comparisons of the one photon and 2PA spectra are shown in Figures 2b-d for each OPEn-NI oligomer in two solvents. Here it can be seen that the bands in the 2PA spectra occur very close

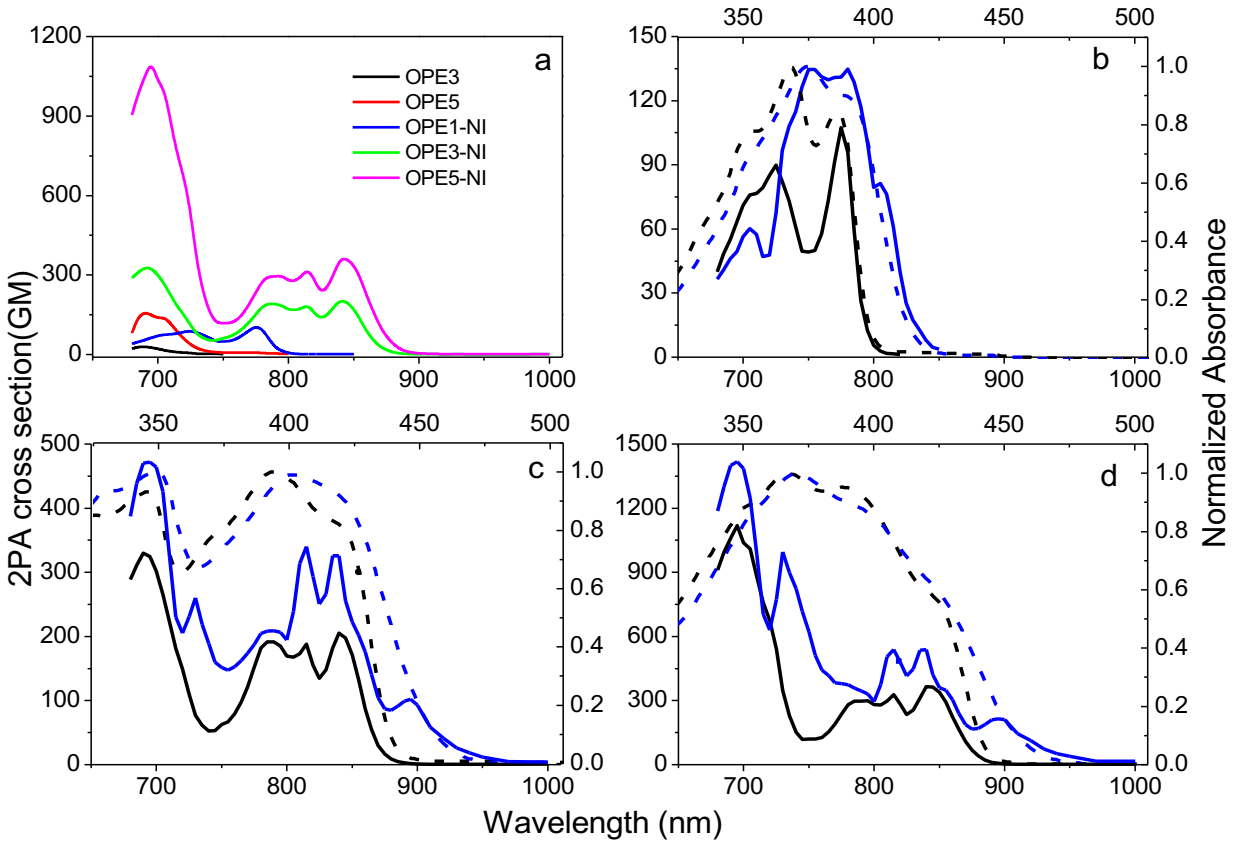

Figure 2. (a) 2PA cross section spectra of OPE and OPEn-NI in hexane. Expanded 2PA cross section (solid lines) and corresponding normalized 1PA (dashed lines) spectra of (b) OPE1-NI, (c) OPE3-NI and (d) OPE5-NI in hexane (black) and DCM (blue). Axis at bottom of each plot is the 2PA wavelength, and the axis at top is the corresponding wavelength in 1-photon (1PA).

to 2λ, where λ is the absorption wavelength in the one photon spectra. It is known that the selection rules are different for one- and two-photon absorption for centrosymmetric molecules.[49] In the OPEn-NI, these selection rules are not expected to be adhered to due to the asymmetry of OPEn-NI chromophores. Due to this, the 2PA transition is expected to be degenerate with the corresponding transition in the one photon spectrum. Thus, the bands in the 2PA spectra at higher energy are likely to be due to the OPE-localized excited state, whereas those at lower energy are due to the OPE to NI charge-transfer state. Moreover, note that the OPEn-NI oligomers exhibit significantly larger σ_{2PA} compared to the OPE model compounds at 690 nm. In OPEn-NI, besides

the extension of conjugation, a highly polarized electronic structure is created by incorporating the NI acceptor, which enhances the σ_{2PA}.[50]

Figure 2b, c and d display the 2PA spectra for OPEn-NI (n = 1, 3 and 5) series in different solvents, DCM and hexane. Compared to hexane, the OPEn-NI chromophores in DCM showed slightly larger σ_{2PA} values. Similar observation were reported for other donor-acceptor systems, and attributed to changes in the electronic structure caused by an increase in the charge separation aided by solvent.[46, 51] Also of interest is that there is an emergence of a clearly resolved feature at low energy in the OPEn-NI 2PA spectra in DCM. The position of this feature mirrors the broadened tail in the corresponding one-photon absorption spectra, and supports the assignment of the lower energy manifold of bands to the OPE to NI charge transfer absorption.

To further investigate the relationship between the CT absorption and the oligomer conjugation length, we calculated the dipole moment difference, $|\Delta\mu_{2PA}|$, between the CT and ground states based on quantitative measurement of the σ_{2PA} according to following equation,[45]

$$|\Delta\mu_{2PA}| = \left(\frac{5}{12\times10^3\pi\ln 10}\frac{nc^2hN_A}{f^2}\frac{\sigma_{2PA}}{\varepsilon_{max}\lambda_{1PA}}\right)^{1/2} \quad (3)$$

where σ_{2PA} is the 2PA cross section (in cm^4 s), c is the speed of light (in cm s^{-1}), h is the Planck constant (in erg s), $f = (n^2 + 2)/3$ is the optical local field correction factor, ε_{max} is the molar extinction coefficient (in M^{-1} cm^{-1}), λ_{1PA} is the 1PA transition wavelength for the CT (in cm), and N_A is Avogadro's number.

Table 2 lists the computed dipole moment difference values for the OPEn-NI. The $|\Delta\mu_{2PA}|$ value obtained turns out to be smallest for OPE1-NI and is larger for OPE3-NI and OPE5-NI. We also calculated the dipole moment difference, $|\Delta\mu_{SS}|$, using the solvatochromic shift method (also called Lippert–Mataga method).[52] In particular, by using equation 2, the dipole moment difference the OPEn-NI can be determined by the correlation of the Stokes shift ($\Delta\nu$) with the orientational

polarizability of each solvent, where v_a and v_e are the CT absorption and CT fluorescence maxima energies, respectively, h is the Planck constant, c is the light speed, r is the molecular Onsager radius, $\Delta\mu$ is the difference between the CT and ground state dipole moments. $f(\varepsilon, n)$ is a function described in equation 4 that depends on the dielectric constant, ε, and the refractive index of solvent, n.

$$\Delta\nu = \nu_a - \nu_e = \frac{2}{hc}\left(\frac{\Delta\mu}{r^3}\right)^2 f(\varepsilon, n) + C \tag{4}$$

$$f(\varepsilon, n) = \left(\frac{\varepsilon-1}{2\varepsilon+1} - \frac{n^2-1}{2n^2+1}\right) \tag{5}$$

Figure 3 shows the plots of the Stokes shifts as a function of the orientational polarizability for the OPEn-NI series, and $|\Delta\mu_{SS}|$ is determined from the slope of the plots. Reasonably linear correlations were obtained for the variations of $\Delta\nu$ *vs* $f(\varepsilon, n)$ (from hexane, ε = 1.89, to DMF, ε =36.7) and the computed values of $|\Delta\mu_{SS}|$ are listed in Table 2.

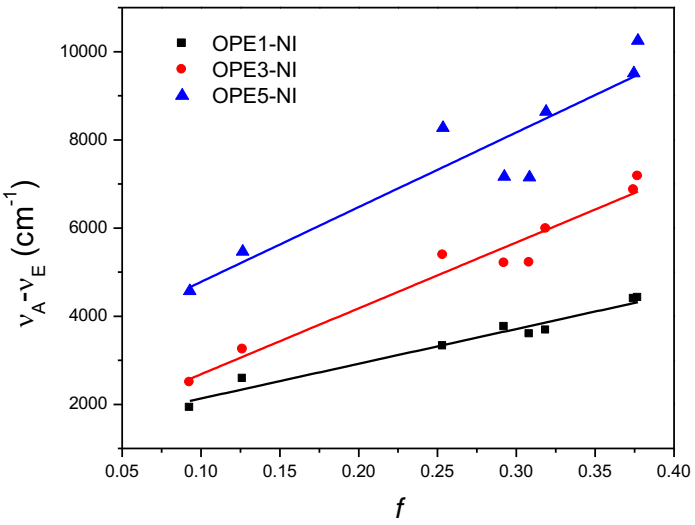

Figure 3. Stokes shifts as a function of the orientational polarizability of OPEn-NI.

Table 2. Difference in dipole moments between the ground and charge-transfer state of OPEn-NI series.

	$\lvert\Delta\mu_{2PA}\rvert$[a] (D)	$\lvert\Delta\mu_{SS}\rvert$[b](D)
OPE1-NI	11	11
OPE3-NI	20	22
OPE5-NI	14	29

[a] Calculated by Equation 1. [c] Calculated by Equation 2.

The large change in the dipole moment in the OPEn-NI reflects the fact that their excited state is much more polar than the ground state. The difference between the ground- and excited-state dipole moments ($\Delta\mu$) is proportional to the degree of charge separation that occurs on photoexcitation. Thus, from the results in Table 2, it is expected that OPE3-NI and OPE5-NI have a higher degree of photoinduced charge separation compared to OPE1-NI and the OPEn oligomers. Comparing the $\Delta\mu$ determined by the two methods, OPE1-NI and OPE3-NI exhibit analogous values. On the other hand, a discrepancy in the values is noted for OPE5-NI. In particular the $\Delta\mu$ obtained from the fluorescence solvatochromism exceeds that determined from the 2PA absorption. A possible explanation for this deviation is related to the fact that the difference dipole deduced by the solvatochromic method is dependent on the Onsager cavity radius, *r*. Onsager theory[53] describe the interaction of solute, placed in a spherical cavity, with the surrounding dielectric medium. Thus, the cavity radius is a parameter that defines how the solvent reaction field is coupled to a point dipole located at the center of the cavity. First, the oligomers herein reported are not spherical, which can cause a discrepancy in *r*, and consequently in $\Delta\mu$. Second, since the donor and acceptor are different in size, it is possible that the point dipole is not located at the cavity center, leading to an overestimation of $\Delta\mu_{SS}$. One the other hand, the $\Delta\mu_{2PA}$ does not depend on the exact location of the charges within the molecule.[38] Thus, the $\Delta\mu_{2PA}$ value for OPE5-NI is consistent with our assumption that upon transition from the ground state to the singlet

excited state the charge distribution responsible for $\Delta\mu$ is mostly localized on the first few repeats of the OPE segment.

Triplet Excited State and Bimolecular Electron Transfer. Nanosecond transient absorption spectra were acquired in THF to study the triplet transient absorption properties of the OPEn series. After excitation, the spectra were dominated by triplet-triplet (TT) absorption as shown in Figure S25. OPE3 showed a TT absorption at about 500 nm, and OPE5 showed a red-shifted TT absorption because of the increasing of conjugation length. This trend has been reported previously for other phenylene ethynylene oligomers.[26, 40] The intensity of the transient absorption decreased with increasing conjugation length, possibly due to a lower intersystem crossing yield for longer oligomers.[26, 44] OPE3-NI and OPE5-NI did not show any transient absorption signals in the nanosecond-microsecond time domain, which indicated the existence of photoinduced charge transfer, and thus quenched the triplet formation.

To gain more insight of the spectra of the reduced state of the OPEn-NI oligomers, a bimolecular photoinduced ET experiment was performed using OPE1-NI as electron acceptor and triethylamine (TEA) as electron donor. Figure 4 depicts nanosecond transient absorption spectra of OPE1-NI in the presence of triethylamine (TEA, c = 5 mM). At early time (50 ns), OPE1-NI showed a transient absorption at about 565 nm which is due to the triplet excited state, which then started to decay. Concomitant to the triplet decay, a new set of bands appeared at 400 - 550 nm. These bands are attributed to the absorption of the anion radical OPE1-NI$^{-\bullet}$ produced by photoinduced ET from TEA to OPE1-NI, as described in Equation 6. The transient absorption peaks at 440 and 480 nm are due to the formation of OPE1-NI radical anion as shown in equation 6.

$$^{3}\text{OPE1-NI}^{*} + \text{TEA} \rightarrow \text{OPE1-NI}^{-\bullet} + \text{TEA}^{+\bullet} \quad (6)$$

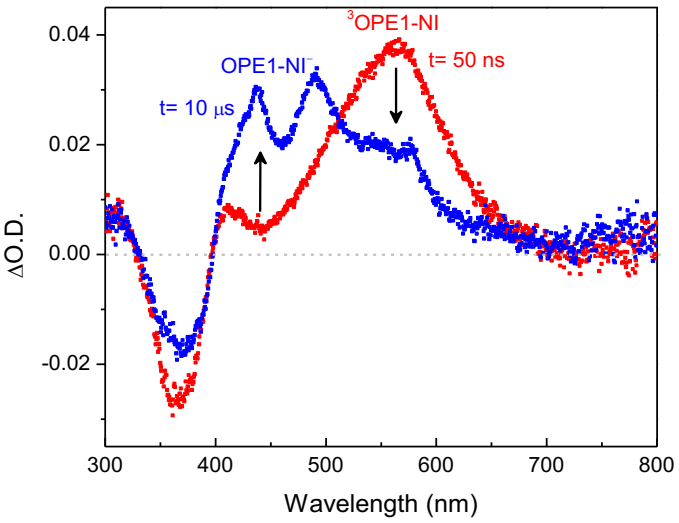

Figure 4. Transient absorption spectra of OPE1-NI with 5 mM TEA in deoxygenated 2:3 acetonitrile/THF solution (λ_{exc} = 355 nm, 4 mJ/ pulse, 50 ns delay (red) and 10 μs (blue) delay).

Intramolecular Photoinduced Electron Transfer in OPEn-NI Oligomers. Femtosecond transient absorption spectroscopy was employed to study the dynamics of photoinduced intramolecular electron transfer in the OPEn-NI oligomers. To better understand the nature of the OPEn-NI dynamics, control experiments were carried out on OPE3 and OPE5 to characterize their excited state absorption (ESA).

The transient absorption of OPE3 and OPE5 in different solvents (hexane, THF and DCM) upon laser excitation are shown in Figure 5 and Supplementary Information. The transient absorption for OPE3 was studied in three solvents (Figure 5a and Figure S26), and in each case it is dominated by a band with maximum absorption at 613 nm at early time.[26] OPE5 (Figure 5b and Figure S26) exhibited a weak stimulated fluorescence at 430-500 nm and two distinct absorptions at 648 and 845 nm. The singlet excited state absorptions for OPE3 and OPE5 are in agreement with previous reports.[40, 42] At longer time delays (t > 3 ns), bands centered at 510 nm for OPE3 and 655 nm for OPE5 appear due to the triplet state. For both oligomers the band closely resembled the triplet-triplet absorption spectra observed by nanosecond-microsecond transient absorption

(Figure S25). Taken together, the solvent dependent transient absorption studies on OPE3 and OPE5 reveal that there is little variation of the spectra for the singlet or triplet states with solvent polarity. The picosecond TA decay dynamics (Table S2) for both oligomers exhibit two components. For OPE3, these two components are possibly due to a fast (~90 ps) and slower (~700 ps) singlet excited state decay. For OPE5, we believe that the fast component (~10 ps) is due to conformational relaxation in the singlet state due to phenylene torsions,[42, 54] and the long component to the singlet excited state decay lifetime, which is in good agreement with the fluorescence lifetime (Table 1).

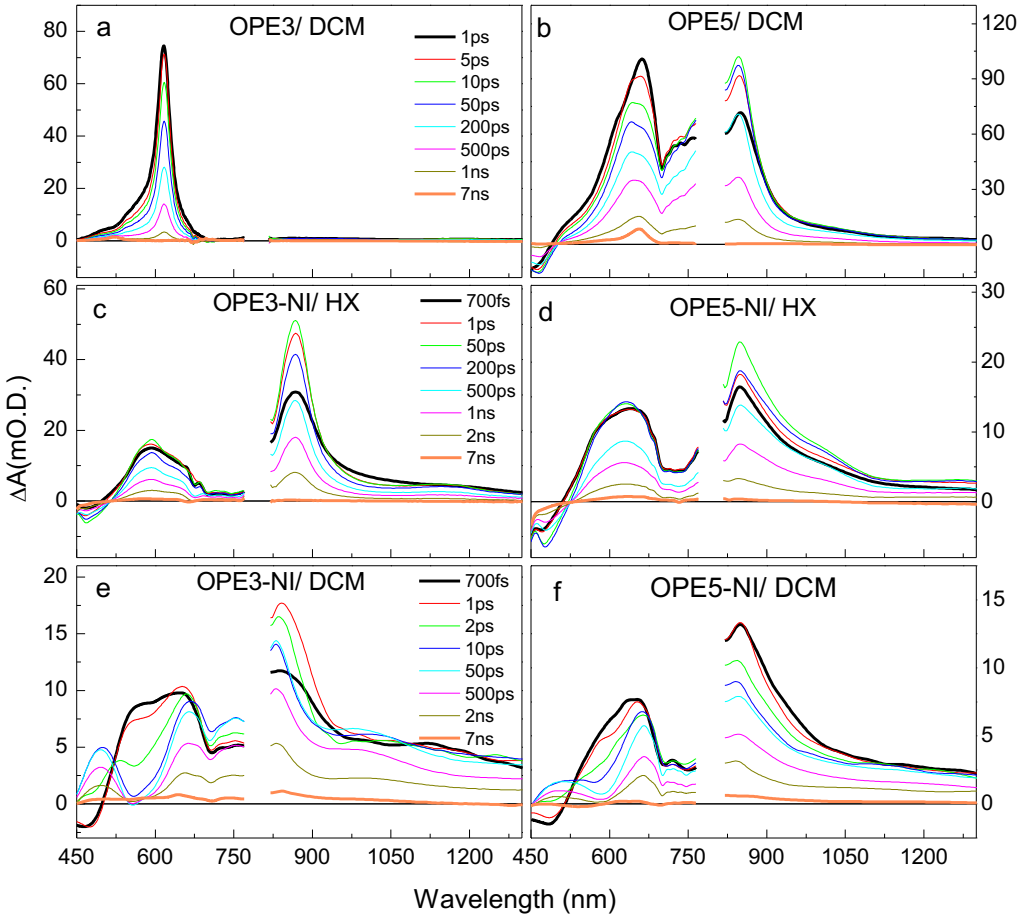

Figure 5. Ultrafast transient absorption spectra of (a) OPE3 in DCM, (b) OPE5 in DCM, (c) OPE3-NI in hexane, (d) OPE5-NI in hexane, (e) OPE3-NI in DCM and (f) OPE5-NI in DCM at the indicated delays following a 340 nm laser excitation pulse for the OPE3 series and at 370 nm for the OPE5 series.

The ultrafast transient absorption spectra for the OPEn-NI oligomers are distinctly different from those of OPEn oligomers. The time evolution of the transient absorption spectra of OPEn-NI (n = 3 and 5) in hexane (Figure 5c and 5d) was measured over a large spectral domain, with two prominent excited-state absorption bands with maxima around 590-635 nm, assigned to the locally excited state absorption of the oligomer, and the second one 850-870 nm, due to delocalization of the excitation into the NI moiety. The excited-state spectra of OPE3-NI and OPE5-NI in polar solvents show notable differences compared to hexane. In DCM (Figure 5e and 5f), as the delay time increased on the 1 - 30 ps time scale, the LE state band around 550-570 nm decays rapidly, and concomitantly new bands around 490 and 650 nm appeared. These bands slowly decayed on the time scale of 50 ps - 7 ns. These absorption features are clearly due to the charge separated state $OPE5^{+\bullet}$-$NI^{-\bullet}$, with the strong band around 490 nm due to the formation of $NI^{-\bullet}$ and at 650 nm to the $OPE^{+\bullet}$.[26]

The transient absorption spectra of OPEn-NI (n= 3 and 5) series reveal major differences in the features with the increase in the donor chain length and solvent polarity. In order to understand the dynamics of charge separation and recombination, the femtosecond transient absorption of OPEn-NI were monitored at 590 nm (Figure 6a and b) and 480 nm (Figure 6c and d), corresponding to the relaxation from a LE state to a CS state and rise of the $NI^{-\bullet}$ absorption, respectively.

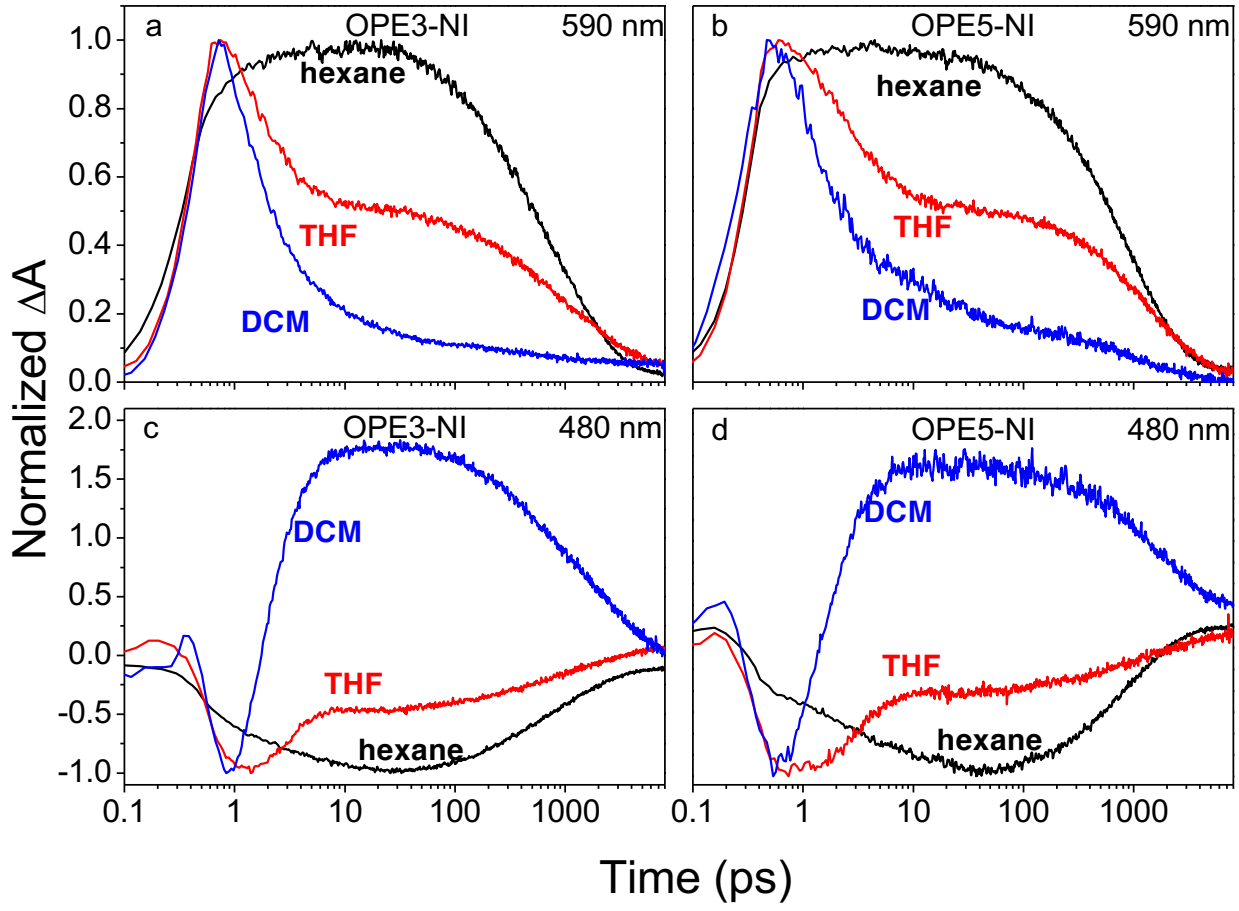

Figure 6. Normalized femtosecond transient absorption kinetics at (a) 590 nm and (c) 480 nm for OPE3-NI and at (b) 590 nm and (d) 480 nm for OPE5-NI in different solvents. The kinetics were normalized by the ΔA values at 480 nm and 590 nm from Figure 5. In each kinetic trace, the maximum value at any time delay was normalized to 1.0 (or -1.0 for traces with negative ΔA values).

Figure 6 shows the time profiles of OPEn-NI in three different solvents (hexane, THF and DCM). The OPEn-NI kinetics traces in hexane were fitted by a biexponential function (Table S2). These two components can be clearly seen in Figure 6a and b as a rising signal followed by a decay component. In hexane the kinetics reflect the formation and decay of one excited state which is attributed to the LE singlet state, with the TA decay dynamics correlating well with the emission decay kinetics in the same solvent (Table 1). It is clear from Figure 6 that the more polar THF and DCM solvents induce a dramatic change in the kinetics associated to the depopulation of the LE

and formation of the CT state. The kinetics in the more polar solvents are represented by a multiexponential fit. The decay traces at 490 nm (Figure 6c and d) associated with formation of the $NI^{-\bullet}$ followed by the charge recombination (in THF and DCM) were fitted with multiple components. The first time constant, τ_1 (Table S2), is an ultrafast component (~1 ps) and can be assigned to the forward electron transfer (ET), while τ_4, is decay of the CT state via charge recombination (~ 1.5 - 2.5 ns). The origin of τ_3 component is not clear, it may be related to structural relaxations in the CT state associated with torsion along the oligo(phenylene ethynylene) chains that influences the stability and delocalization of the (+) charge (polaron) that resides on the conjugated segment. The considerable increase in the forward ET rates in the more polar solvents is attributed to the increase of driving force for ET from the locally excited state. This point will be explored more fully below through energetics calculations. The forward ET rates slightly decrease as the oligomer length increased. However, the dynamics for charge recombination are dependent on oligomer length, with an increase between OPE1-NI and OPE3-NI, followed by a decrease to OPE5-NI.

Energetics for Photoinduced Electron Transfer and Charge Recombination. To understand the effect of donor conjugation length on the ET driving force, electrochemical experiments were conducted to estimate the energetics for all members of the series. The electrochemical results (Figure S29) and excitation energies are summarized in Table S3. The driving force, ΔG_{CS}, of the charge separation in the OPEn-NI compounds in a series of solvents was estimated by equation 7:[28, 55]

$$\Delta G_{CS} = e[E_{ox} - E_{red}] - E_{00} - \frac{e^2}{4\pi\epsilon_0\varepsilon_s R_{DA}} - \left[\frac{e^2}{8\pi\epsilon_0} - \left(\frac{1}{r^+} + \frac{1}{r^-}\right)\left(\frac{1}{\varepsilon_{ref}} - \frac{1}{\varepsilon_s}\right)\right] \quad (7)$$

where the driving force of electron transfer, ΔG_{CS}, is given by the difference between the oxidation potential of the OPE donor, E_{ox}, the reduction potential of the NI acceptor, E_{red}, the zero-zero

transition energy, E_{00}, calculated from the absorption and emission spectra of the LE state in hexane solution, and the Columbic correction term. In the latter term, e is the charge of an electron, ε_{ref} is the dielectric constant of the solvent used in electrochemical measurement (DCM, 8.93), ε_s is the dielectric constant of the solvent and R_{DA} is the center-to-center distance between donor and acceptor units, which was calculated from DFT B3LYP 6-31G* (Figure S30), ϵ_0 is vacuum permittivity and r^+ and r^- are the radii of the positive and negative ions.

Figure 7 shows the correlation of driving force, ΔG_{CS} , as a function of solvent dielectric constant, ε. The estimated ΔG_{CS} values on the electron transfer from OPEn-NI (n = 3 and 5) to give $OPEn^{\bullet+}$-$NI^{\bullet-}$ are negative in all the solvents, indicating that ET is exothermic. However, note that the process is only weakly exothermic in hexane and becomes considerably more exothermic in THF and DCM. This explains the observations from the spectroscopic studies, which suggest that ET is slow in the non-polar hydrocarbon solvent. Interestingly, the obtained values of driving force for OPEn-NI (n = 3 and 5) are in excellent agreement with the energy of the CT emission as calculated from the spectra in Figure 1 (Table S4).

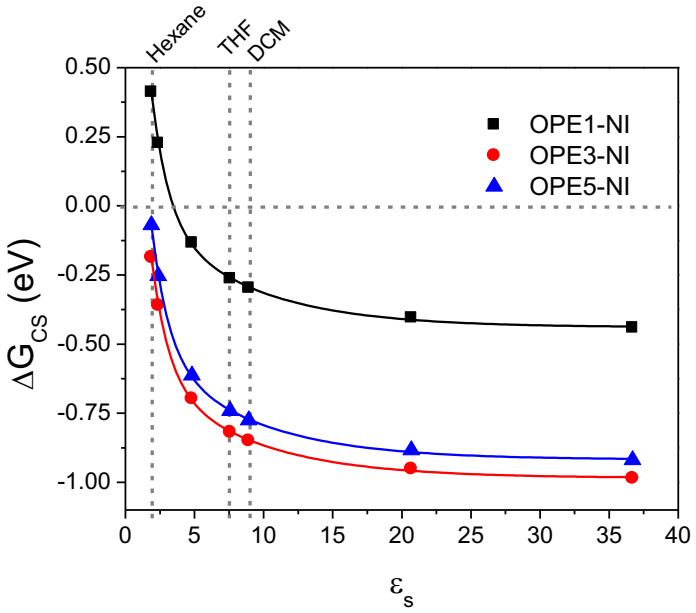

Figure 7. Driving force (ΔG) for the photoinduced charge separation in OPEn-NI oligomers as a function of the solvent dielectric constant. ΔG_{CS} values were estimated by using equation 7.

Discussion

This study investigated the effect of incorporation of the 1,8-naphthalimide electron acceptor on the photophysics of a set of three oligo(phenylene ethynylene)s. The goal of the study was to examine photoinduced electron transfer where the OPE acts as the donor, and the NI moiety is the acceptor. Previous work has demonstrated that when electron donating substituents are linked to the 4-position of the NI moiety the compounds exhibit charge transfer (CT) absorption and fluorescence.[32-36] Comparison of the absorption spectra of the of the OPEn-NI series with the parent OPEs reveals significant differences due to the NI acceptor (Figure 1). In particular, OPE3-NI features a distinct, red-shifted CT absorption band that is solvatochromic. In OPE5-NI a CT absorption band overlaps with the locally excited (LE) absorption of the phenylene ethylyene oligomer. The assignment of the absorption bands to CT is augmented by the 2-photon absorption spectra (Figure 2), where it can be clearly seen that the CT bands are distinct and enhanced in 2-photon. Each of the OPEn-NI oligomers exhibits a broad, red-shifted fluorescence, the energy of which varies strongly with solvent as expected for CT state.

A key objective of this work was to explore whether the variation in conjugation length of the phenylene ethynylene oligomer gives rise to differences in the energy or structure of the CT excited state. The key question is whether extending the conjugation length of the "donor" OPE segment gives rise to a difference in the structure and dynamics of the CT state. A previous study of a series of oligo(thiophene)s linked to the NI acceptor showed that the energy of the CT state continuously decreased with increasing length of the oligo(thiophene) up to eight thiophene repeat units. This suggested that in the CT state, $(T_n)^+$-NI^-, the hole (+) that is on the oligothiophene

segment is stabilized by delocalization across the entire oligomer segment. In the present study of the OPEn-NI series, the spectroscopic and dynamics results suggest that there are relatively small differences in the degree of CT in OPE3-NI and OPE5-NI. In particular, the CT emission is only slightly red-shifted in the longer oligomer, the 2-photon absorption spectra in the CT region are very similar (750 – 950 nm, Fig. 2), and the transient absorption spectra and dynamics in the more polar solvents (THF and DCM) are closely similar. Taken together, we interpret the results as suggesting that structure of the CT state, $OPEn^{\bullet+}$-$NI^{\bullet-}$, is similar in the two oligomers, with the hole (+) that resides on the OPE segment being mainly localized on the first three phenylene ethynylene repeats as suggested by Scheme 1. Apparently, the extra stabilization of the hole (+) that would be provided by delocalization across the entire oligomer is not sufficient to overcome the Coulombic binding energy in the CT state that localizes the charge in proximity to the NI acceptor.

Scheme 1. Photoinduced electron transfer process in OPE3-NI and OPE5-NI oligomers.

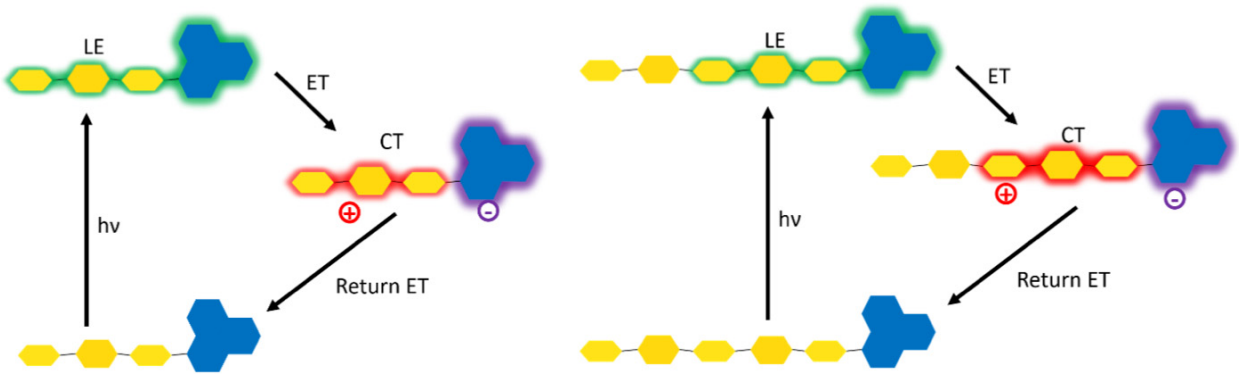

Summary and Conclusions

This work has explored the photophysics of a series of oligo(phenylene ethynylene) oligomers that feature a 1,8-naphthalene imide acceptor moiety linked to the oligomer terminus. The

properties are compared carefully with a series of oligomers that lack the NI acceptor. The results reveal that the NI acceptor exhibits a profound change in the photophysical properties, especially in moderately polar solvents. The fluorescence and ultrafast transient absorption results indicate that initial excitation produces a locally excited state, but this state rapidly undergoes a transition to a charge transfer state, where the OPE segment acts as the donor and the NI is the acceptor. Comparison of the photophysical properties of the oligomers with different lengths suggests that the structure of the CT state is not strongly influenced by conjugation length. This leads to the conclusion that the hole (+) is relatively localized on the first three ethynylene units in the CT state.

Supporting Information Available: Complete details concerning the synthesis and characterization of the compounds, NMR spectra, fluorescence spectra in different solvents, nanosecond transient absorption spectra, additional femtosecond transient absorption spectra, femtosecond transient absorption lifetime data, cyclic voltammograms, table comparing calculated and experimental CT state energies, DFT calculated oligomer structures with D-A distances.

Acknowledgments

We acknowledge the National Science Foundation for support of this work (Grant No. CHE-1904288). We also acknowledge C. Jason Zeman, IV for calculation of the structures and center-to-center distances and Yan Zhao for contributing to the synthetic work.

References

1. Wasielewski, M. R., Photoinduced Electron-Transfer in Supramolecular Systems for Artificial Photosynthesis. *Chem. Rev.* **1992,** *92*, 435-461.

2. Gust, D.; Moore, T. A.; Moore, A. L., Molecular Mimicry of Photosynthetic Energy and Electron-Transfer. *Acc. Chem. Res.* **1993,** *26*, 198-205.
3. Choi, M. S.; Yamazaki, T.; Yamazaki, I.; Aida, T., Bioinspired Molecular Design of Light-Harvesting Multiporphyrin Arrays. *Angew. Chem. Int. Ed.* **2004,** *43*, 150-158.
4. Barber, J., Photosynthetic Energy Conversion: Natural and Artificial. *Chem. Soc. Rev.* **2009,** *38*, 185-196.
5. Bonaccorso, F.; Colombo, L.; Yu, G. H.; Stoller, M.; Tozzini, V.; Ferrari, A. C.; Ruoff, R. S.; Pellegrini, V., Graphene, Related Two-Dimensional Crystals, and Hybrid Systems for Energy Conversion and Storage. *Science* **2015,** *347*, 1246501.
6. Jakowetz, A. C.; Bohm, M. L.; Zhang, J.; Sadhanala, A.; Huettner, S.; Bakulin, A. A.; Rao, A.; Friend, R. H., What Controls the Rate of Ultrafast Charge Transfer and Charge Separation Efficiency in Organic Photovoltaic Blends. *J. Am. Chem. Soc.* **2016,** *138*, 11672-11679.
7. Vandewal, K.; Mertens, S.; Benduhn, J.; Liu, Q., The Cost of Converting Excitons into Free Charge Carriers in Organic Solar Cells. *J. Phys. Chem. Lett.* **2020,** *11*, 129-135.
8. Closs, G. L.; Miller, J. R., Intramolecular Long-Distance Electron-Transfer in Organic-Molecules. *Science* **1988,** *240*, 440-447.
9. Paddonrow, M. N., Investigating Long-Range Electron-Transfer Processes with Rigid, Covalently-Linked Donor-(Norbornylogous Bridge)-Acceptor Systems. *Acc. Chem. Res.* **1994,** *27*, 18-25.
10. Williams, R. M.; Zwier, J. M.; Verhoeven, J. W., Photoinduced Intramolecular Electron-Transfer in a Bridged C-60 (Acceptor) Aniline (Donor) System - Photophysical Properties of the First Active Fullerene Diad. *J. Am. Chem. Soc.* **1995,** *117*, 4093-4099.

11. Guldi, D. M.; MAggini, M.; Scorrano, G.; Prato, M., Intramolecular Electron Transfer in Fullerene/Ferrocene Based Donor−Bridge−Acceptor Dyads. *J. Am. Chem. Soc.* **1997,** *119*, 974-980.

12. Bredas, J. L.; Beljonne, D.; Coropceanu, V.; Cornil, J., Charge-Transfer and Energy-Transfer Processes in pi-Conjugated Oligomers and Polymers: A Molecular Picture. *Chem. Rev.* **2004,** *104*, 4971-5003.

13. Albinsson, B.; Eng, M. P.; Pettersson, K.; Winters, M. U., Electron and Energy Transfer in Donor-Acceptor systems with conjugated molecular bridges. *PCCP* **2007,** *9*, 5847-5864.

14. Huang, F.; Chen, K. S.; Yip, H. L.; Hau, S. K.; Acton, O.; Zhang, Y.; Luo, J. D.; Jen, A. K. Y., Development of New Conjugated Polymers with Donor−π-Bridge−Acceptor Side Chains for High Performance Solar Cells. *J. Am. Chem. Soc.* **2009,** *131*, 13886–13887.

15. Ricks, A. B.; Solomon, G. C.; Colvin, M. T.; Scott, A. M.; Chen, K.; Ratner, M. A.; Wasielewski, M. R., Controlling Electron Transfer in Donor-Bridge-Acceptor Molecules Using Cross-Conjugated Bridges. *J. Am. Chem. Soc.* **2010,** *132*, 15427-15434.

16. Vasilev, A. A.; De Mey, K.; Asselberghs, I.; Clays, K.; Champagne, B.; Angelova, S. E.; Spassova, M. I.; Li, C.; Mullen, K., Enhanced Intramolecular Charge Transfer in New Type Donor-Acceptor Substituted Perylenes. *J. Phys. Chem. C* **2012,** *116*, 22711-22719.

17. Li, G. Q.; Govind, N.; Ratner, M. A.; Cramer, C. J.; Gagliardi, L., Influence of Coherent Tunneling and Incoherent Hopping on the Charge Transfer Mechanism in Linear Donor-Bridge-Acceptor Systems. *J. Phys. Chem. Lett.* **2015,** *6*, 4889-4897.

18. Gilbert, M.; Albinsson, B., Photoinduced Charge and Energy Transfer in Molecular Wires. *Chem. Soc. Rev.* **2015,** *44*, 845-862.

19. Schubert, C.; Margraf, J. T.; Clark, T.; Guldi, D. M., Molecular Wires - Impact of pi-Conjugation and Implementation of Molecular Bottlenecks. *Chem. Soc. Rev.* **2015,** *44*, 988-998.

20. Liu, C.; Wang, K.; Gong, X.; Heeger, A. J., Low Bandgap Semiconducting Polymers for Polymeric Photovoltaics. *Chem. Soc. Rev.* **2016,** *45*, 4848-4849.

21. Zhang, J.; Xu, W.; Sheng, P.; Zhao, G. Y.; Zhu, D. B., Organic Donor-Acceptor Complexes as Novel Organic Semiconductors. *Acc. Chem. Res.* **2017,** *50*, 1654-1662.

22. Miura, T.; Carmieli, R.; Wasielewski, M. R., Time-Resolved EPR Studies of Charge Recombination and Triplet-State Formation within Donor-Bridge-Acceptor Molecules Having Wire-Like Oligofluorene Bridges. *J. Phys. Chem. A* **2010,** *114*, 5769-5778.

23. Jones, A. L.; Gish, M. K.; Zeman, C. J.; Papanikolas, J. M.; Schanze, K. S., Photoinduced Electron Transfer in Naphthalene Diimide End-Capped Thiophene Oligomers. *J. Phys. Chem. A* **2017,** *121*, 9579-9588.

24. Giacalone, F.; Segura, J. L.; Martin, N.; Guldi, D. M., Exceptionally Small Attenuation Factors in Molecular Wires. *J. Am. Chem. Soc.* **2004,** *126*, 5340-5341.

25. Wiberg, J.; Guo, L. J.; Pettersson, K.; Nilsson, D.; Ljungdahl, T.; Martensson, J.; Albinsson, B., Charge Recombination versus Charge Separation in Donor−Bridge−Acceptor Systems. *J. Am. Chem. Soc.* **2007,** *129*, 155-163.

26. Jiang, J.; Alsam, A.; Wang, S.; Aly, S. M.; Pan, Z.; Mohammed, O. F.; Schanze, K. S., Effect of Conjugation Length on Photoinduced Charge Transfer in pi-Conjugated Oligomer-Acceptor Dyads. *J. Phys. Chem. A* **2017,** *121*, 4891-4901.

27. Loi, M. A.; Troisi, A., Charge Generation Mechanism in Organic Solar Cells. *Phys. Chem. Chem. Phys.* **2014,** *16*, 20277-20278.

28. van Hal, P. A.; Knol, J.; Langeveld-Voss, B. M. W.; Meskers, S. C. J.; Hummelen, J. C.; Janssen, R. A. J., Photoinduced Energy and Electron Transfer in Fullerene-Oligothiophene-Fullerene Triads. *J. Phys. Chem. A* **2000,** *104*, 5974-5988.

29. Zhao, Y.; Shirai, Y.; Slepkov, A. D.; Cheng, L.; Alemany, L. B.; Sasaki, T.; Hegmann, F. A.; Tour, J. M., Synthesis, Spectroscopic and Nonlinear Optical Properties of Multiple [60]Fullerene–Oligo(p-phenylene ethynylene) Hybrids. *Chem. Eur. J* **2005,** *11*, 3643-3658.

30. Guo, F. Q.; Ogawa, K.; Kim, Y. G.; Danilov, E. O.; Castellano, F. N.; Reynolds, J. R.; Schanze, K. S., A Fulleropyrrolidine End-Capped Platinum-Acetylide Triad: The Mechanism of Photoinduced Charge Transfer in Organometallic Photovoltaic Cells. *Phys. Chem. Chem. Phys.* **2007,** *9*, 2724-2734.

31. Gish, M. K.; Jones, A. L.; Papanikolas, J. M.; Schanze, K. S., Role of Structure in Ultrafast Charge Separation and Recombination in Naphthalene Diimide End-Capped Thiophene Oligomers. *J Phys Chem C* **2018,** *122*, 18802-18808.

32. Asaoka, S.; Takeda, N.; Iyoda, T.; Cook, A. R.; Miller, J. R., Electron and Hole Transport To Trap Groups at the Ends of Conjugated Polyfluorenes. *J. Am. Chem. Soc.* **2008,** *130*, 11912-11920.

33. Zaikowski, L.; Mauro, G.; Bird, M.; Karten, B.; Asaoka, S.; Wu, Q.; Cook, A. R.; Miller, J. R., Charge Transfer Fluorescence and 34 nm Exciton Diffusion Length in Polymers with Electron Acceptor End Traps. *J. Phys. Chem. B* **2015,** *119*, 7231-7241.

34. Zhang, J. C.; Li, G. W.; Kang, C.; Lu, H.; Zhao, X. X.; Li, C. H.; Li, W. H.; Bo, Z. S., Synthesis of Star-Shaped Small Molecules Carrying Peripheral 1,8-Naphthalimide Functional Groups and their Applications in Organic Solar Cells. *Dyes Pigments* **2015,** *115*, 181-189.

35. Jin, Z. N.; Li, N. J.; Wang, C. F.; Jiang, H. J.; Lu, J. M.; Zhou, Q. H., Synthesis and Fluorescence Property of Some Novel 1,8-Naphthalimide Derivatives Containing a Thiophene Ring at the C-4 Position. *Dyes Pigments* **2013,** *96*, 204-210.

36. Jones, A. L.; Schanze, K. S., Fluorescent Charge-Transfer Excited States in Acceptor Derivatized Thiophene Oligomers. *J. Phys. Chem. A* **2020,** *124*, 7001-7013.

37. Makarov, N. S.; Drobizhev, M.; Rebane, A., Two-Photon Absorption Standards in the 550-1600 nm Excitation Wavelength Range. *Opt. Express* **2008,** *16*, 4029-4047.

38. Rebane, A.; Drobizhev, M.; Makarov, N. S.; Beuerman, E.; Haley, J. E.; Krein, D. M.; Burke, A. R.; Flikkema, J. L.; Cooper, T. M., Relation between Two-Photon Absorption and Dipolar Properties in a Series of Fluorenyl-Based Chromophores with Electron Donating or Electron Withdrawing Substituents. *J. Phys. Chem. A* **2011,** *115*, 4255-4262.

39. de Reguardati, S.; Pahapill, J.; Mikhailov, A.; Stepanenko, Y.; Rebane, A., High-Accuracy Reference Standards for Two-Photon Absorption in the 680-1050 nm Wavelength Range. *Opt. Express* **2016,** *24*, 9053-9066.

40. Sudeep, P. K.; James, P. V.; Thomas, K. G.; Kamat, P. V., Singlet and Triplet Excited-State Interactions and Photochemical Reactivity of Phenyleneethynylene Oligomers. *J. Phys. Chem. A* **2006,** *110*, 5642-5649.

41. Matsunaga, Y.; Takechi, K.; Akasaka, T.; Ramesh, A. R.; James, P. V.; Thomas, K. G.; Kamat, P. V., Excited-State and Photoelectrochemical Behavior of Pyrene-Linked Phenyleneethynylene Oligomer. *J. Phys. Chem. B* **2008,** *112*, 14539-14547.

42. Duvanel, G.; Grilj, J.; Schuwey, A.; Gossauer, A.; Vauthey, E., Ultrafast Excited-State Dynamics of Phenyleneethynylene Oligomers in Solution. *Photochem. Photobiol. Sci.* **2007,** *6*, 956-963.

43. Tang, Y.; Hill, E. H.; Zhou, Z.; Evans, D. G.; Schanze, K. S.; Whitten, D. G., Synthesis, Self-Assembly, and Photophysical Properties of Cationic Oligo(p-phenyleneethynylene)s. *Langmuir* **2011,** *27*, 4945-4955.

44. Tang, Y.; Corbitt, T. S.; Parthasarathy, A.; Zhou, Z.; Schanze, K. S.; Whitten, D. G., Light-Induced Antibacterial Activity of Symmetrical and Asymmetrical Oligophenylene Ethynylenes. *Langmuir* **2011,** *27*, 4956-4962.

45. Mikhaylov, A.; Uudsemaa, M.; Trummal, A.; Arias, E.; Moggio, I.; Ziolo, R.; Cooper, T. M.; Rebane, A., Spontaneous Symmetry Breaking Facilitates Metal-to-Ligand Charge Transfer: A Quantitative Two-Photon Absorption Study of Ferrocene-phenyleneethynylene Oligomers. *J. Phys. Chem. Lett.* **2018,** *9*, 1893-1899.

46. Chung, S. J.; Rumi, M.; Alain, V.; Barlow, S.; Perry, J. W.; Marder, S. R., Strong, Low-Energy Two-Photon Absorption in Extended Amine-Terminated Cyano-Substituted Phenylenevinylene Oligomers. *J. Am. Chem. Soc.* **2005,** *127*, 10844-10845.

47. Zhang, Y.; Jiang, M.; Han, G. C.; Zhao, K.; Tang, B. Z.; Wong, K. S., Solvent Effect and Two-Photon Optical Properties of Triphenylamine-Based Donor−Acceptor Fluorophores. *J Phys Chem C* **2015,** *119*, 27630–27638.

48. Xu, C.; Webb, W. W., Measurement of Two-photon Excitation Cross Sections of Molecular Fluorophores with Data from 690 to 1050 nm. *J. Opt. Soc. Am. B: Opt. Phys.* **1996,** *13*, 481-491.

49. Pawlicki, M.; Collins, H. A.; Denning, R. G.; Anderson, H. L., Two-Photon Absorption and the Design of Two-Photon Dyes. *Angew. Chem. Int. Ed.* **2009,** *48*, 3244-3266.

50. Aratani, N.; Kim, D.; Osuka, A., pi-Conjugation Enlargement Toward the Creation of Multi-Porphyrinic Systems with Large Two-Photon Absorption Properties. *Chem.: Asian J* **2009,** *4*, 1172-1182.

51. Tan, Y.; Zhang, Q.; Yu, J.; Zhao, X.; Tian, Y.; Cui, Y.; Hao, X.; Yang, Y.; Qian, G., Solvent Effect on Two-Photon Absorption (TPA) of Three Novel Dyes with Large TPA Cross-Section and Red Emission. *Dyes Pigments* **2012,** *97*, 58-64.

52. Lippert, E., Dipolmoment Und Elektronenstruktur Von Angeregten Molekulen. *Z. Naturforsch. A* **1955,** *10*, 541-545.

53. Onsager, L., Electric Moments of Molecules in Liquids. *J. Am. Chem. Soc.* **1936,** *58*, 1486-1493.

54. Sluch, M. I.; Godt, A.; Bunz, U. H. F.; Berg, M. A., Excited-State Dynamics of Oligo(p-phenyleneethynylene): Quadratic Coupling and Torsional Motions. *J. Am. Chem. Soc.* **2001,** *123*, 6447-6448.

55. Weller, A., Photoinduced Electron Transfer in Solution: Exciplex and Radical Ion Pair Formation Free Enthalpies and their Solvent Dependence. *Z. Phys. Chem.* **1982,** *133*, 93-98.

TOC Graphic